ERICE PREPRINT SERIES

«ETTORE MAJORANA» CENTRE FOR SCIENTIFIC CULTURE

Su 9402

EMCSC/93-07
19 December 1993

ENERGY AND SCALE DEPENDENCE OF HEAVY QUARK PRODUCTION IN QCD

G. Anzivino[4], F. Arzarello[2], G. Bari[2], M. Basile[2,8], L. Bellagamba[2], D. Boscherini[2], G. Bruni[2], P. Bruni[2], G. Cara Romeo[2], M. Chiarini[2,12], L. Cifarelli[2,9], F. Cindolo[2], F. Ciralli[2], A. Contin[1,2], M. Dardo[5,11], S. D'Auria[2], C. Del Papa[2,8], S. De Pasquale[4], F. Frasconi[2], P. Giusti[2], G. Iacobucci[2], Liu Wenje[3,7,12], G. Maccarrone[4], A. Margotti[2], T. Massam[2], R. Nania[2], S. Qian[2,12], G. Sartorelli[2,8], Yu. M. Shabelski[3,10,12], O. P. Strogova[3,6,12], R. Timellini[2,12], L. Votano[4] and A. Zichichi[1,2]

1) CERN, Geneva, Switzerland
2) INFN, Bologna, Italy
3) INFN, Eloisatron Project, Erice, Italy
4) INFN, LNF, Frascati, Italy
5) INFN, Torino, Italy
6) INP, Moscow State University, Moscow, Russia
7) Istitute of Mechanics, Beijing, China
8) Physics Department, University of Bologna, Italy
9) Physics Department, University of Pisa, Italy
10) PNPI, Gatchina, St. Petersburg, Russia
11) II Faculty of Science, University of Torino, Alessandria, Italy
12) World Laboratory, Lausanne, Switzerland

Abstract

We consider the energy dependence of charm and beauty production cross-sections in pp or $\overline{p}p$ collisions up to $\sqrt{s} = 200$ TeV for different values of the scale μ^2, using different proton structure functions. The cross-sections are computed accounting for leading order and next-to-leading order perturbative QCD contributions. The values of K-factors increase significantly with the energy for relatively small scale values, $\mu^2 \approx M^2$, where M is the heavy quark mass, and do not practically depend on the energy for higher values, $\mu^2 = 4M^2 \div 8M^2$. The calculated cross-sections as functions of the energy for different values of μ^2 have a common crossing point if the gluon structure functions used have proper Altarelli-Parisi μ^2-evolution. The same holds true when considering the energy and scale dependence of the heavy quark cross-sections in high-energy photoproduction.

(Submitted to Il Nuovo Cimento)

EMCSC - via Guarnotta 26, Erice, 91026 Italy - tel. (923) 869133, fax. (923) 869226

1. INTRODUCTION

Perturbative QCD calculations [1, 2] for heavy quark production cross-sections in hadron-hadron collisions account for leading-order (LO) $O(\alpha_s^2)$ as well as next-to-leading order (NLO) $O(\alpha_s^3)$ contributions. The standard QCD expression has the form:

$$\sigma(s) = \sum_{i,j} \int \hat{\sigma}(x_1 x_2 s, M^2, \mu^2) \cdot G_i(x_1, \mu^2) \cdot G_j(x_2, \mu^2) dx_1 dx_2, \qquad (1)$$

where $G_i(x_1, \mu^2)$ and $G_j(x_2, \mu^2)$ are the distributions of partons i and j inside the colliding hadrons and $\hat{\sigma}(x_1 x_2 s, M^2, \mu^2)$ is the cross-section for heavy quark pair production in the parton-parton subprocess.

The heavy quark production cross-sections depend essentially on the value of the scale μ^2 since all quantities, namely the parton distributions G_i and G_j, the QCD coupling α_s and the parton-parton cross-section $\hat{\sigma}(x_1 x_2 s, M^2, \mu^2)$, depend on μ^2. In principle the scale values for structure functions, α_s coupling, LO and NLO matrix elements can be different but usually they are all assumed to be the same for simplicity. Two different possibilities to choose the value of μ^2 were discussed in the literature. One of them corresponds to the "minimal sensitivity" [3] of the cross-section with respect to μ^2, i.e. to the condition $d\sigma/d\mu^2 = 0$, and the other to the "fastest convergence" [4] of the cross-section, i.e. to the condition K = 1, where the K-factor is defined as:

$$K = \frac{\sigma(LO) + \sigma(NLO)}{\sigma(LO)}. \qquad (2)$$

Unfortunately the detailed analysis of [2] shows that both variants give the same value of μ^2 in the case of very large quark masses (top production) and both do not work in the case of beauty production. Up to now we cannot account for higher order contributions $O(\alpha_s^4)$. On the other hand the K-factor values obtained in the case of pp ($\bar{p}p$) collisions are usually equal [5] to 2÷3, showing that high order contributions can be essential.

In the present work we study the energy dependence of K-factors for heavy flavour (charm and beauty) hadroproduction with different parton structure functions and at different values of the scale μ^2 (section 2). Then we consider the energy behaviour of heavy quark hadroproduction cross-sections, whose values strongly depend on the explicit form of parton structure functions, again for different μ^2 scales (section 3). We repeat the same exercise also for heavy quark photoproduction cross-sections, whose NLO QCD corrections are comparatively small (section 4). Summary and conclusion are presented in section 5.

2. ENERGY AND SCALE DEPENDENCE OF K-FACTORS IN HEAVY FLAVOUR HADROPRODUCTION

We account for both leading-order (LO, $gg \to Q\overline{Q}$ and $q\bar{q} \to Q\overline{Q}$) $O(\alpha_s^2)$ and next-to-leading order (NLO, $gg \to Q\overline{Q}g$, $q\bar{q} \to Q\overline{Q}g$, $gq \to qQ\overline{Q}$, etc.) $O(\alpha_s^3)$ contributions to the heavy quark production cross-section for different parton structure functions, namely two Duke-Owens sets [6], DO1 and DO2, two "old", GRV1 (GRV(LO)) and GRV2 (GRV(HO)) [7], and two "new", GRV3 (GRV(LO)) and GRV4 (GRV(HO)) [8], Gluck-Reya-Vogt sets and four Morfin-Tung sets [9], MT1, MT2, MT3 and MT4 (S-DIS, E-DIS, B1-DIS and B2-DIS).

Let us first compare the results of our calculations with the experimental data in terms of total cross-sections for charm and beauty production in pp or $\overline{p}p$ collisions[1]. For charm we use a relatively small scale value, $\mu^2 = 4$ GeV^2 (because DO as well as MT structure functions are determined only for $\mu^2 \geq 4$ GeV^2), together with a relatively large value, $\mu^2 = 8M^2$ (where M is the heavy quark mass, i.e. $M = M_c = 1.5$ GeV). Analogously for beauty we use $\mu^2 = M^2$ and $8M^2$, with $M = M_b = 4.7$ GeV. One can see from table 1 that the experimental cross-sections for $c\overline{c}$ production at low energies ($\sqrt{s} = 27$ GeV [10] and $\sqrt{s} = 39$ GeV [11], pp) are in reasonable agreement with the calculations at $\mu^2 = 4$ GeV^2, while a significant disagreement appears at $\mu^2 = 8M_c^2$. At higher energy ($\sqrt{s} = 630$ GeV, $\overline{p}p$), the experimental data [12, 13] for both $c\overline{c}$ and $b\overline{b}$ production, are in reasonable agreement with the calculations except when GRV1 structure functions are used.

In figs. 1 and 2 we present the K-factor energy dependence for beauty production in $p\overline{p}$ collisions at different scale values, $\mu^2 = M_b^2$, $4M_b^2$ and $8M_b^2$ (curves 1, 2 and 3, respectively). In all cases, curve 1 increases with energy, while curves 2 and 3 stay nearly flat. Analogous results for charm production are shown in figs. 3 and 4, for $\mu^2 = 4$ GeV^2, $4M_c^2$ and $8M_c^2$ (curves 1, 2 and 3), and the situation is similar: contrary to curves 2 and 3, curve 1 rapidly grows with $\sqrt{s}$.

3. ENERGY AND SCALE DEPENDENCE OF HEAVY QUARK HADROPRODUCTION CROSS-SECTIONS

Let us now consider the LO+NLO QCD predictions for the total heavy quark cross-sections at high energies. These strongly depend on the choice of structure functions. Nevertheless they show some interesting features when calculated using different scales μ^2.

In figs. 5 and 6 we present the total cross-section vs. $\sqrt{s}$ for beauty production in $\overline{p}p$ collisions at $\mu^2 = 0.4M_b^2, M_b^2$, $4M_b^2$ and $8M_b^2$ (curves 1, 2, 3 and 4), using all the different sets of structure functions listed in section 2. In all cases, except for MT4 structure functions, the curves have a common crossing point or crossing points which are very close to each other. In the case of DO structure functions (constant for gluons at $\mu^2 = \mu_0^2$ and $x \to 0$), the crossing point is at comparatively low energies, while for all the other structure functions (having a singularity for gluons at $x \to 0$), it is shifted towards higher energies. Notice that for GRV and MT sets, curves 3 and 4 are almost undistinguishable. The same cross-section curves for charm production are shown in figs.

1) At high and superhigh energies, the particle-production processes in pp or $\overline{p}p$ collisions are essentially the same. The present QCD calculations, presented in section 2 and 3, are obtained for $\overline{p}p$ collisions.

7 and 8: their general features are essentially the same as for beauty production (figs. 5 and 6).

The existence of a crossing point of the cross-section curves vs. $\sqrt{s}$ at different μ^2 is directly connected with an analogous crossing point of the gluon distribution[2)] curves when these are considered as functions of x for different μ^2. At relatively large x-values ($\geq$ 0.1), the gluon structure function decreases with increasing μ^2 and at smaller x-values it increases. So at small $\sqrt{s}$ (when only relatively large x-values contribute), the cross-section decreases as μ^2 increases. When $\sqrt{s}$ increases, smaller values of x begin to contribute. Therefore the cross-sections for heavy quark production have a faster increase with $\sqrt{s}$ at larger values of μ^2. This results in the observed crossing point. In the case of "non-singular" (DO) structure functions, the region of integration over x_1, x_2 in eq. (1) giving an essential contribution to the cross-section is larger than for "singular" (MT, GRV) structure functions. This is why the crossing points for "non-singular" structure functions appear at lower energy. On the other hand, the fact that all curves have a common crossing point is not trivial since the parton-parton cross-section also depends on μ^2.

Let us try to understand what is the difference between set MT4 and all the other sets of structure functions. In fig. 9a we present the gluon distributions of sets MT3 and MT4 at μ^2 = 4 GeV^2 and 100 GeV^2. There is a significant difference in the behaviour of these distributions at small x. In the case of MT3, the ratio ($xG(x, \mu^2$ = 100 GeV^2)/($xG(x, \mu^2$ = 4 GeV^2)), i.e. (curve 2 / curve 1) in fig. 9a, increases with decreasing x, which is in agreement with Altarelli-Parisi evolution. However the same ratio in the case of MT4 is practically constant at $x < 0.001$, in contradiction with the evolution law and such behaviour results in the absence of crossing points in figs. 6 and 8. To illustrate this point in fig. 9b we present the cross-section vs. $\sqrt{s}$ for $b\bar{b}$ production in $\bar{p}p$ collisions at the same four μ^2 values used so far, for a toy gluon distribution:

$$xG(x, \mu^2) \propto (1-x)^7 \tag{3}$$

which has a satisfactory x-dependence but does not depend on μ^2. In this case too there is no crossing point of the curves with different μ^2.

Notice that if we use very large values of μ^2, say up to 1000 GeV^2 (which is however unlike for $c\bar{c}$ or $b\bar{b}$ production), the common crossing point disappears although there is still a region of energy where the scale dependence of the heavy flavour cross-sections is weak. As far as the expected t-quark production cross-section is concerned, in the wide range of possible top masses, a weak scale dependence is obtained for $\mu^2 = M_t^2 \div 8M_t^2$.

Some predictions for charm and beauty production cross-sections at high and superhigh energies (corresponding to Tevatron, LHC, SSC and Eloisatron (ELN) colliders) are presented in table 2 for $\mu^2 = 8M^2$.

2) Valence and sea quark contributions to heavy flavour production cross-sections at high energies are small, i.e. less than 10 $\div$ 20%.

4. ENERGY AND SCALE DEPENDENCE OF HEAVY QUARK PHOTOPRODUCTION CROSS-SECTIONS

In heavy flavour photoproduction, the LO diagram ($\gamma g \to Q\overline{Q}$) [14, 15] gives the main contribution while NLO corrections are relatively small [16-18]. In addition the ratio $\sigma(NLO)/\sigma(LO)$ decreases when using a gluon structure function with a singularity at $\mu^2 = \mu_0^2$ and $x \to 0$ because the relative contribution at very small x becomes more important. The LO cross-section of heavy quark pair production in γp interactions has the form [14, 15]:

$$\sigma(s) = \int \hat{\sigma}(xs, M^2, \mu^2) \cdot G(x, \mu^2) dx, \tag{4}$$

where $G(x, \mu^2)$ is the gluon structure function of the target.

The results for charm production cross-section calculations with DO1, MT1 and GRV4 structure functions, at three (for DO1 and MT1) and at four (for GRV4) different values of μ^2, are presented in fig. 10 together with the experimental data which are taken from [19]. The agreement is reasonable with GRV4 and MT1 at small μ^2, but not with DO1 which produces a too weak energy dependence.

Predictions for beauty photoproduction are presented in figs. 11 and 12 at four different values of μ^2 and for ten different sets of structure functions (as in sections 2 and 3). The qualitative behaviour of the curves is similar to the case of figs. 5 and 6: the curves at different μ^2 have a common crossing point except for MT4 gluon structure function. The same situation appears for charm photoproduction cross-sections in figs. 13 and 14 (to be compared with figs. 7 and 8).

Finally it is also worth considering the ratio of $b\bar{b}$ to $c\bar{c}$ cross-sections, since some experimental as well as theoretical uncertainties disappear in this case. This ratio also depends on the scale, as shown in fig. 15, but its dependence on structure functions becomes weaker at larger μ^2.

5. CONCLUSION

In heavy quark hadroproduction, relatively large scale values, i.e. $\mu^2 = 4M_Q^2 \div 8M_Q^2$, give the weakest energy ($\sqrt{s}$) dependence of K-factors for all sets of structure functions (DO, GRV and MT, see section 2) considered herein, in the range $\sqrt{s}$ = 100 GeV $\div$ 200 TeV. At the same time, the charm and beauty cross-section calculations with LO and NLO contributions turn out to better agree with existing experimental data at relatively high energy ($\sqrt{s}$ = 630 GeV, $\overline{p}p$) rather than at low energy ($\sqrt{s}$ = 27 and 39 GeV, pp). With smaller scale values, i.e. $\mu^2 \approx M_Q^2$, the calculated cross-sections show a fair overall agreement with the experimental data at different energies but the K-factors in this case depend significantly on the initial energy. Of course it could be that even the scale μ^2 actually depends on the energy. In this respect, future measurements of heavy flavour cross-sections will indeed be very interesting.

In addition, in both pp or $\overline{p}p$ and γp interactions, the heavy quark production cross-sections, which strongly depend on parton structure functions, have different $\sqrt{s}$-

evolutions at different values of μ^2, in a wide μ^2 region (from $0.4M_Q^2$ up to $8M_Q^2$). However, if the structure functions used in the calculations evolve vs. μ^2 at small x "à la" Altarelli-Parisi, there is an energy corresponding to a common crossing point among the various cross-section curves obtained at different μ^2 (or to crossing points which are very close to each other) where the heavy flavour cross-section does not depend on the scale. At this particular energy, the theoretical calculations have a smaller number of uncertainties and a detailed comparison with experimental results may illustrate the role of non-perturbative or high-order diagram contributions with better accuracy.

ACKNOWLEGEMENTS

We are grateful to G. Altarelli, Ya. I. Azimov, V. A. Khoze, A. D. Martin and M. G. Ryskin for useful and stimulating discussions.

Table 1: QCD predictions for the total cross-sections (in μb) of charm and beauty hadroproduction compared with experimental data.

$\sqrt{s}$	27 GeV, $c\bar{c}$		39 GeV, $c\bar{c}$		630 GeV, $c\bar{c}$		630 GeV, $b\bar{b}$	
μ^2	4 GeV^2	$8M^2$	4 GeV^2	$8M^2$	4 GeV^2	$8M^2$	M^2	$8M^2$
DO1	15	8	26	17	278	338	16	14
DO2	30	15	46	28	416	728	27	23
GRV1	10	4	24	11	2920	1970	30	18
GRV2	10	5	23	13	1530	1100	24	15
GRV3	10	5	21	12	1710	1290	24	15
GRV4	13	7	28	16	1500	1090	26	16
MT1	14	7	33	17	872	604	22	15
MT2	11	6	25	14	587	430	17	12
MT3	11	6	25	15	764	542	21	14
MT4	9	4	20	11	1140	798	19	13
Experiment	14÷23		29÷55		680±560±250±210		19.3±7±9	

Table 2: QCD predictions for the total cross-sections (in mb) of charm and beauty production in high energy $\bar{p}p$ interactions at $\mu^2 = 8M^2$.

$\sqrt{s}$	1.8 TeV		16 TeV		40 TeV		200 TeV	
	$c\bar{c}$	$b\bar{b}$	$c\bar{c}$	$b\bar{b}$	$c\bar{c}$	$b\bar{b}$	$c\bar{c}$	$b\bar{b}$
DO1	0.76	0.055	3.4	0.71	6.2	1.9	16.6	10.6
DO2	2.0	0.12	15.3	3.0	34.6	10.8	140	98.1
GRV1	8.0	0.11	95.3	2.4	238	7.4	1060	43.8
GRV2	3.4	0.073	25.1	0.98	52.0	2.5	169	10.7
GRV3	4.8	0.084	48.6	1.5	115	4.4	462	23.8
GRV4	3.3	0.075	23.7	0.97	48.5	2.4	155	10.3
MT1	1.4	0.052	6.8	0.44	12.7	0.95	36.6	3.4
MT2	0.95	0.041	4.2	0.31	7.6	0.64	20.8	2.2
MT3	1.2	0.050	4.5	0.37	7.4	0.76	16.9	2.4
MT4	2.8	0.058	33.7	0.90	95.8	2.6	602	16.2

Figure captions

Fig. 1 : Energy dependence of K-factor with DO and GRV structure functions for $b\bar{b}$ production in $p\bar{p}$ collisions at $\mu^2 = M_b^2$ (curve 1), $4M_b^2$ (curve 2) and $8M_b^2$ (curve 3).

Fig. 2 : Energy dependence of K-factor with MT structure functions for $b\bar{b}$ production in $p\bar{p}$ collisions at $\mu^2 = M_b^2$ (curve 1), $4M_b^2$ (curve 2) and $8M_b^2$ (curve 3).

Fig. 3 : Energy dependence of K-factor with DO and GRV structure functions for $c\bar{c}$ production in $p\bar{p}$ collisions at $\mu^2 = 4$ GeV^2 (curve 1), $4M_c^2$ (curve 2) and $8M_c^2$ (curve 3).

Fig. 4 : Energy dependence of K-factor with MT structure functions for $c\bar{c}$ production in $p\bar{p}$ collisions at $\mu^2 = 4$ GeV^2 (curve 1), $4M_c^2$ (curve 2) and $8M_c^2$ (curve 3).

Fig. 5 : Energy dependence of $b\bar{b}$ production cross-section in $p\bar{p}$ collisions at $\mu^2 = 0.4M_b^2$ (curve 1), M_b^2 (curve 2), $4M_b^2$ (curve 3) and $8M_b^2$ (curve 4) with DO and GRV structure functions.

Fig. 6 : Energy dependence of $b\bar{b}$ production cross-section in $p\bar{p}$ collisions at $\mu^2 = 0.4M_b^2$ (curve 1), M_b^2 (curve 2), $4M_b^2$ (curve 3) and $8M_b^2$ (curve 4) with MT structure functions.

Fig. 7 : Energy dependence of $c\bar{c}$ production cross-section in $p\bar{p}$ collisions at $\mu^2 = 4$ GeV^2 (curve 1), $4M_c^2$ (curve 2) and $8M_c^2$ (curve 3) for DO and GRV structure functions.

Fig. 8 : Energy dependence of $c\bar{c}$ production cross-section in $p\bar{p}$ collisions at $\mu^2 = 4$ GeV^2 (curve 1), $4M_c^2$ (curve 2) and $8M_c^2$ (curve 3) for MT structure functions.

Fig. 9 : MT3 (solid line) and MT4 (dashed line) gluon structure functions vs. x at $\mu^2 = 4$ GeV^2 (curve 1) and 100 GeV^2 (curve 2) (a); energy dependence of $b\bar{b}$ production cross-section in $p\bar{p}$ collisions for the gluon distribution of eq. (3) at $\mu^2 = 0.4M_b^2$ (curve 1), M_b^2 (curve 2), $4M_b^2$ (curve 3) and $8M_b^2$ (curve 4) (b).

Fig. 10 : Energy dependence of $c\bar{c}$ production cross-section in γp interactions at $\mu^2 = M_c^2$ (curve 1), 4 GeV^2 (curve 2), $4M_c^2$ (curve 3) and $8M_c^2$ (curve 4) for DO1, MT1 and GRV4 structure functions, compared with experimental results.

Fig. 11 : Energy dependence of $b\bar{b}$ production cross-section in γp interactions at $\mu^2 = 0.4M_b^2$ (curve 1), M_b^2 (curve 2), $4M_b^2$ (curve 3) and $8M_b^2$ (curve 4) with DO and GRV structure functions.

Fig. 12 : Energy dependence of $b\bar{b}$ production cross-section in γp interactions at $\mu^2 = 0.4M_b^2$ (curve 1), M_b^2 (curve 2), $4M_b^2$ (curve 3) and $8M_b^2$ (curve 4) with MT structure functions.

Fig. 13 : Energy dependence of $c\bar{c}$ production cross-section in γp interactions at $\mu^2 = 4$ GeV^2 (curve 1), $4M_c^2$ (curve 2) and $8M_c^2$ (curve 3) with DO and GRV structure functions.

Fig. 14 : Energy dependence of $c\bar{c}$ production cross-section in γp interactions at $\mu^2 = 4$ GeV^2 (curve 1), $4M_c^2$ (curve 2) and $8M_c^2$ (curve 3) with MT structure functions.

Fig. 15 : Energy dependence of $b\bar{b}$ to $c\bar{c}$ cross-section ratio in γp interactions at $\mu^2 = 4$ GeV^2 for charm and $\mu^2 = M_b^2$ for beauty (curve 1), and at $\mu^2 = 8M_c^2$ for charm and $\mu^2 = 8M_b^2$ for beauty (curve 2), with different (DO1, MT1 and GRV4) structure functions.

REFERENCES

[1] P. Nason, S. Dawson and R. K. Ellis, Nucl. Phys. B303 (1988) 607.
[2] G. Altarelli et al., Nucl. Phys. B308 (1988) 724.
[3] P. M. Stevenson, Phys. Rev. D23 (1981) 2916.
[4] G. Grunberg, Phys. Rev. D29 (1984) 2315.
[5] I. Sarcevic, P. Carruthers and Q. Gao, Phys. Rev. D40 (1989) 3600.
[6] D. W. Duke and J. F. Owens, Phys. Rev. D30 (1984) 49.
[7] M. Gluck, E. Reya and A. Vogt, Z. Phys. C48 (1990) 471.
[8] M. Gluck, E. Reya and A. Vogt, Z. Phys. C53 (1992) 127.
[9] J. G. Morfin and W.-K. Tung, Z. Phys. C52 (1991) 13.
[10] M. Aguilar-Benitez et al., Z. Phys. C40 (1988) 321.
[11] R. Ammar et al., Phys. Lett. B183 (1987) 110.
[12] O. Botner et al., Phys. Lett. B236 (1990) 488.
[13] C. Albajar et al., Phys. Lett. B256 (1991) 121.
[14] H. Fritzsch and K.-H. Streng, Phys. Lett. B72 (1978) 385.
[15] L. N. Jones and H. W. Wyld, Phys. Rev. D17 (1978) 759.
[16] M. Drees and K. Grassie, Z. Phys. C28 (1985) 451.
[17] R. K. Ellis and Z. Kunszt, Nucl. Phys. B303 (1988) 653.
[18] A. Levy, preprint DESY 92-073 (1992).
[19] R. W. Forty, Proc. of the XXIV Int. Conf. on High Energy Physics, Munich, Germany, 4-10 August 1989 (ed. by R. Kotthaus and I.H. Kuhn, Springer-Verlag Berlin, Heidelberg, 1989), p. 669.

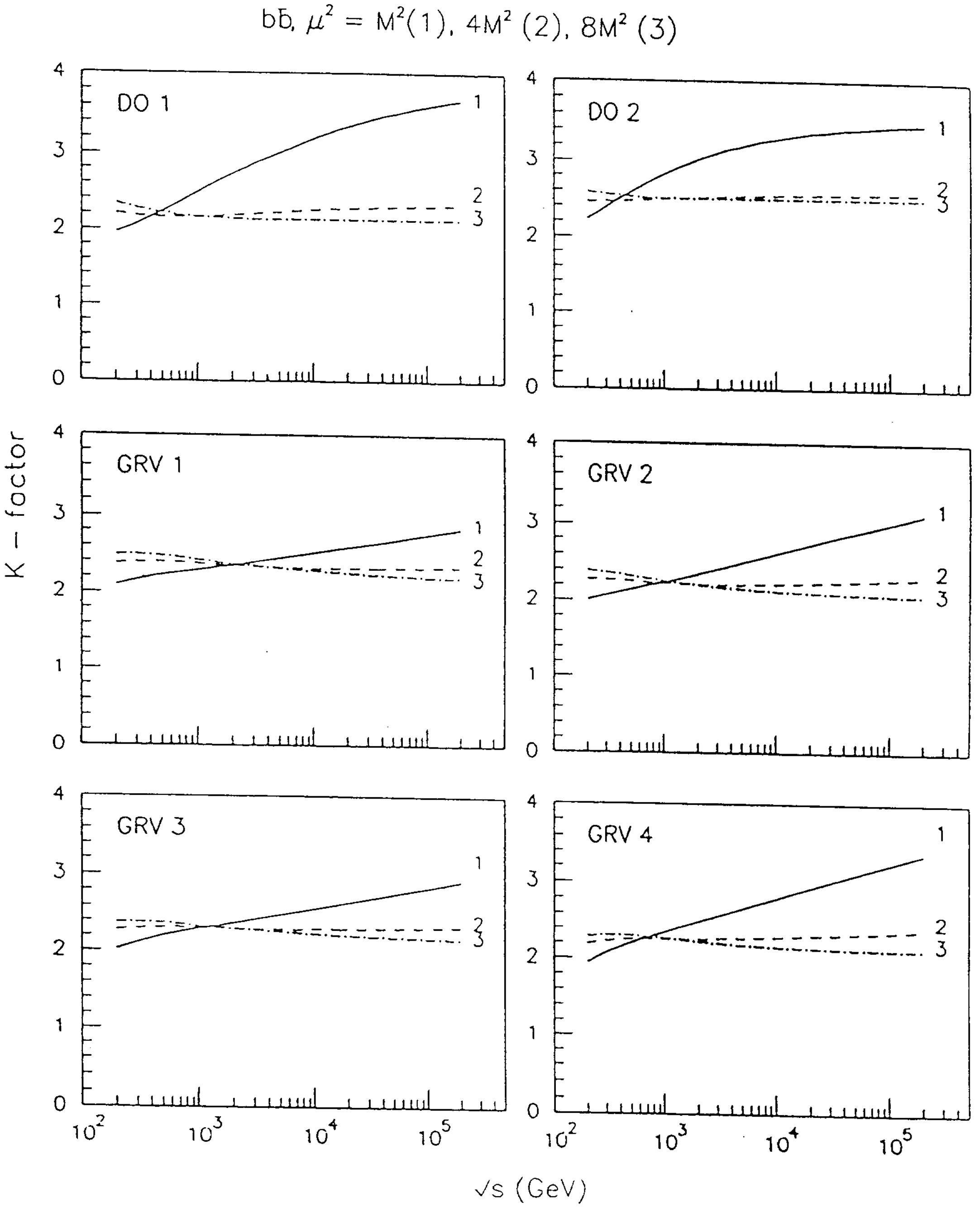
bb̄, μ² = M²(1), 4M² (2), 8M² (3)
DO 1
DO 2
GRV 1
GRV 2
GRV 3
GRV 4
1
2
3
K – factor
√s (GeV)
0
1
2
3
4
10²
10³
10⁴
10⁵

Fig. 1

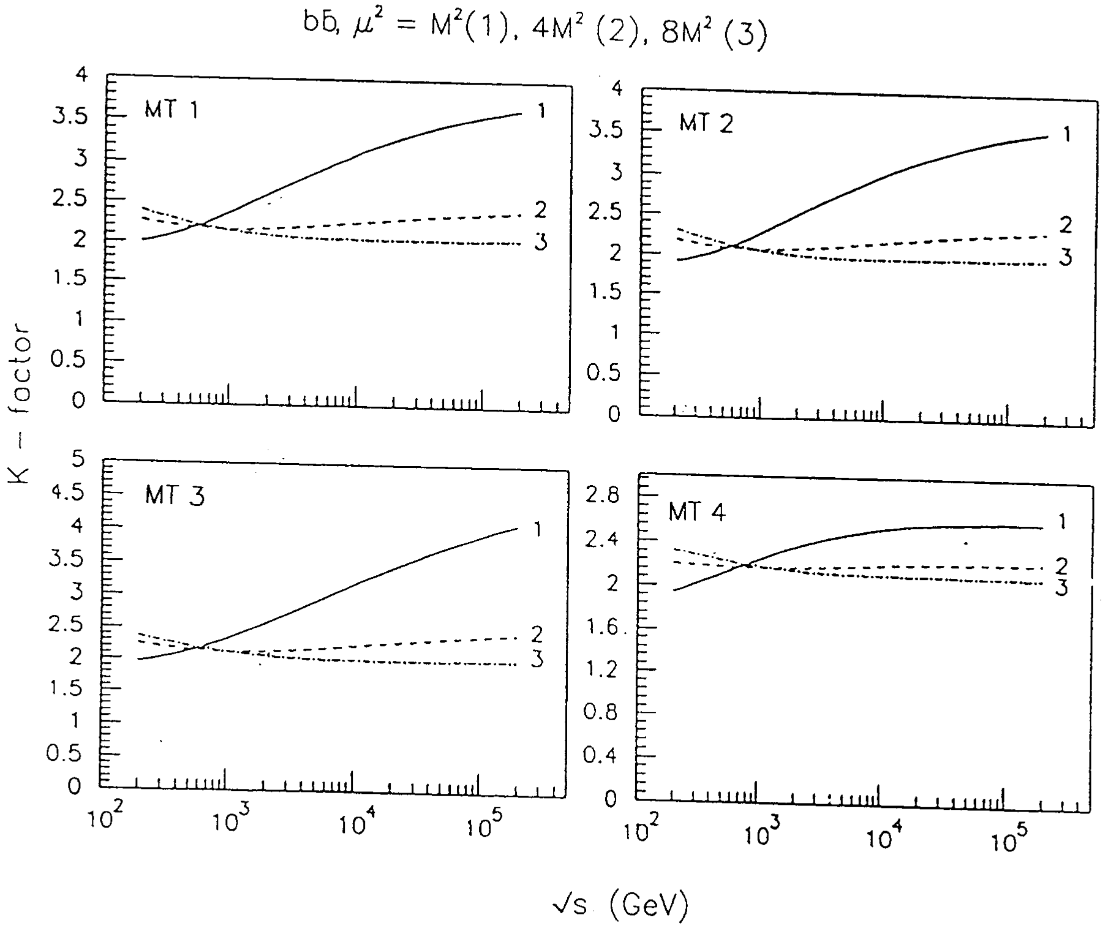

Fig.2

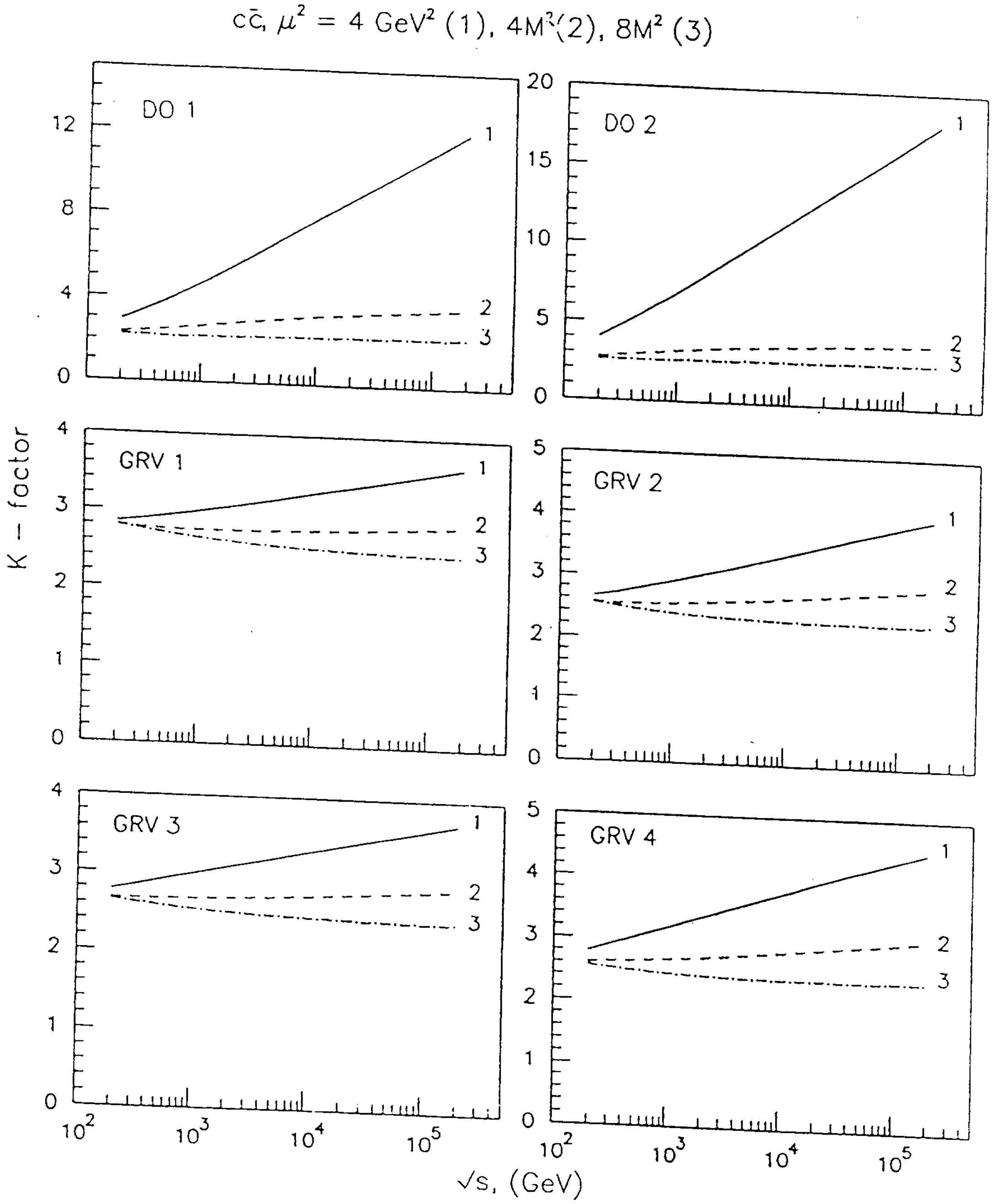
cc̄, μ² = 4 GeV² (1), 4M² (2), 8M² (3)
DO 1
DO 2
GRV 1
GRV 2
GRV 3
GRV 4
K – factor
√s, (GeV)
1
2
3

Fig.3

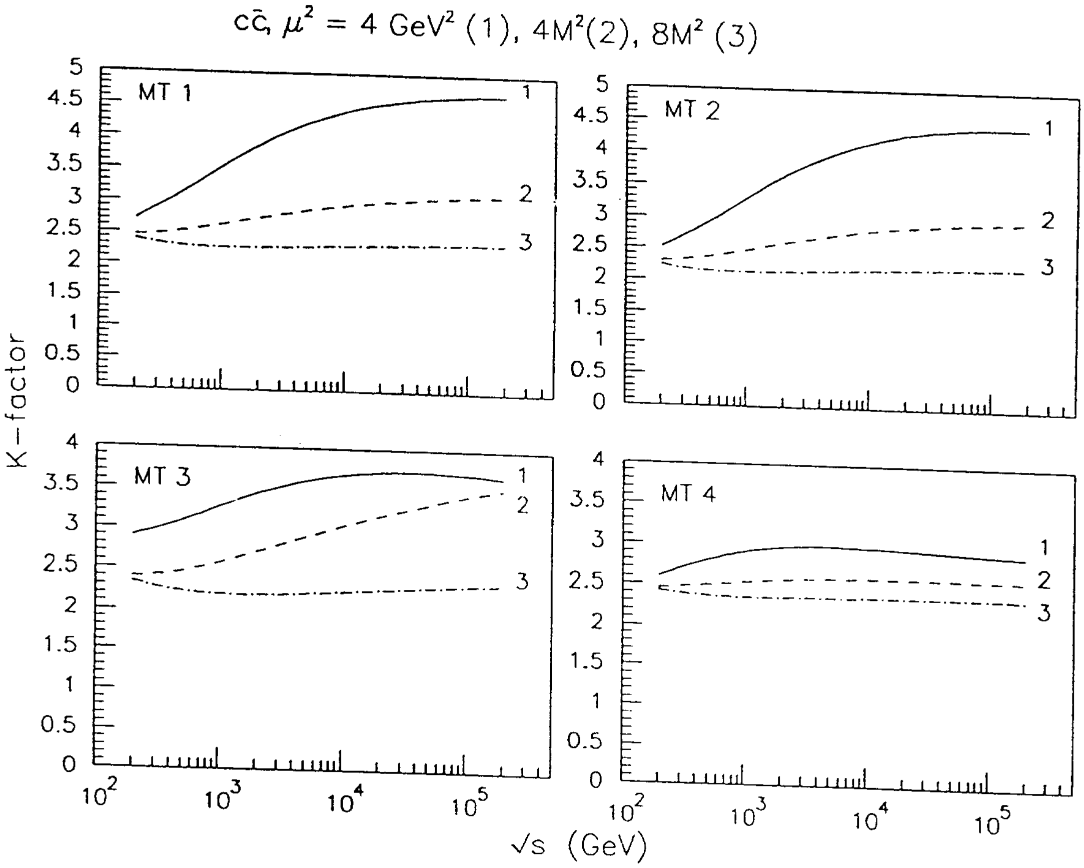

Fig.4

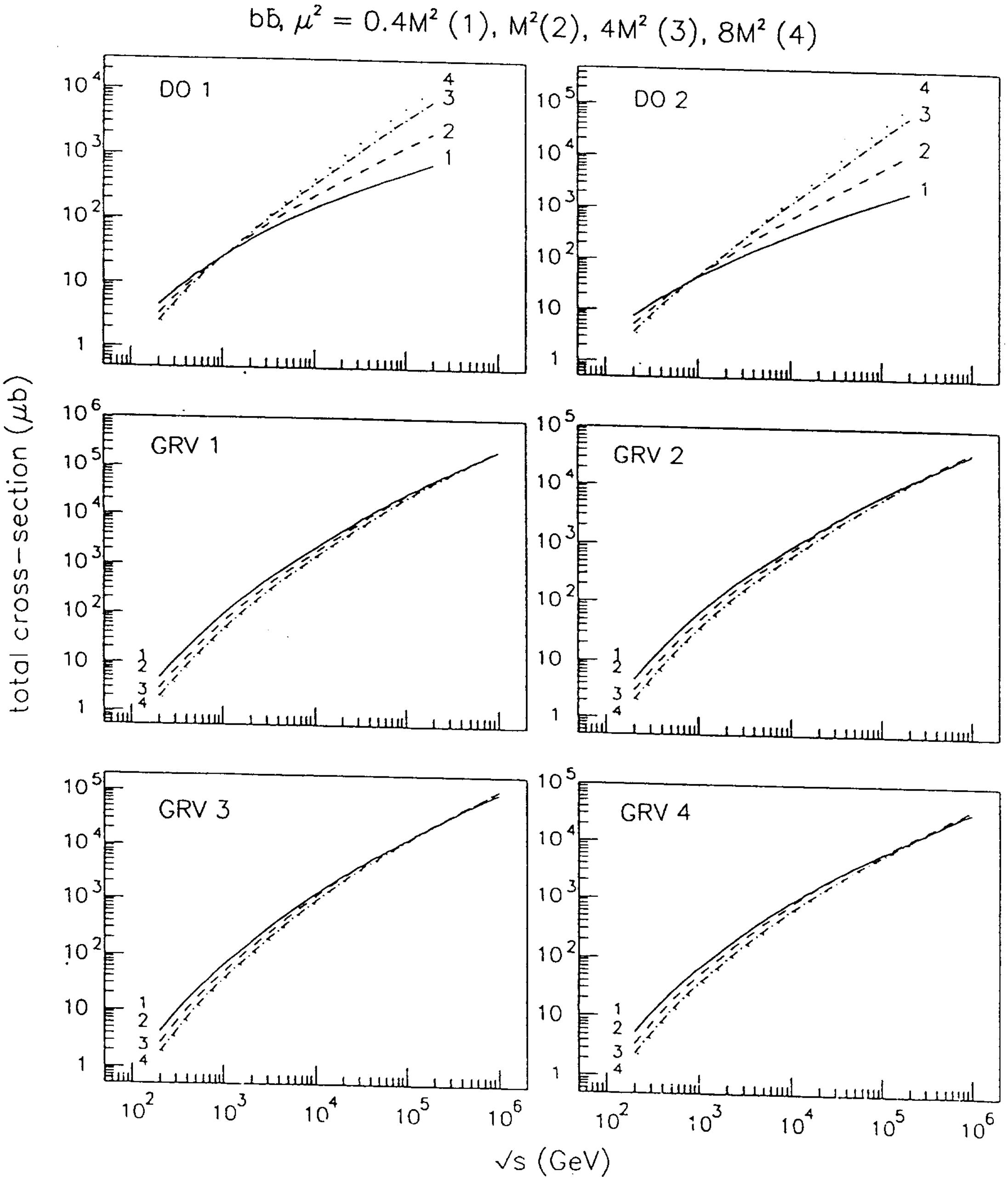
bb̄, μ^2 = 0.4M² (1), M²(2), 4M² (3), 8M² (4)
DO 1
DO 2
GRV 1
GRV 2
GRV 3
GRV 4
total cross-section (μb)
√s (GeV)

Fig.5

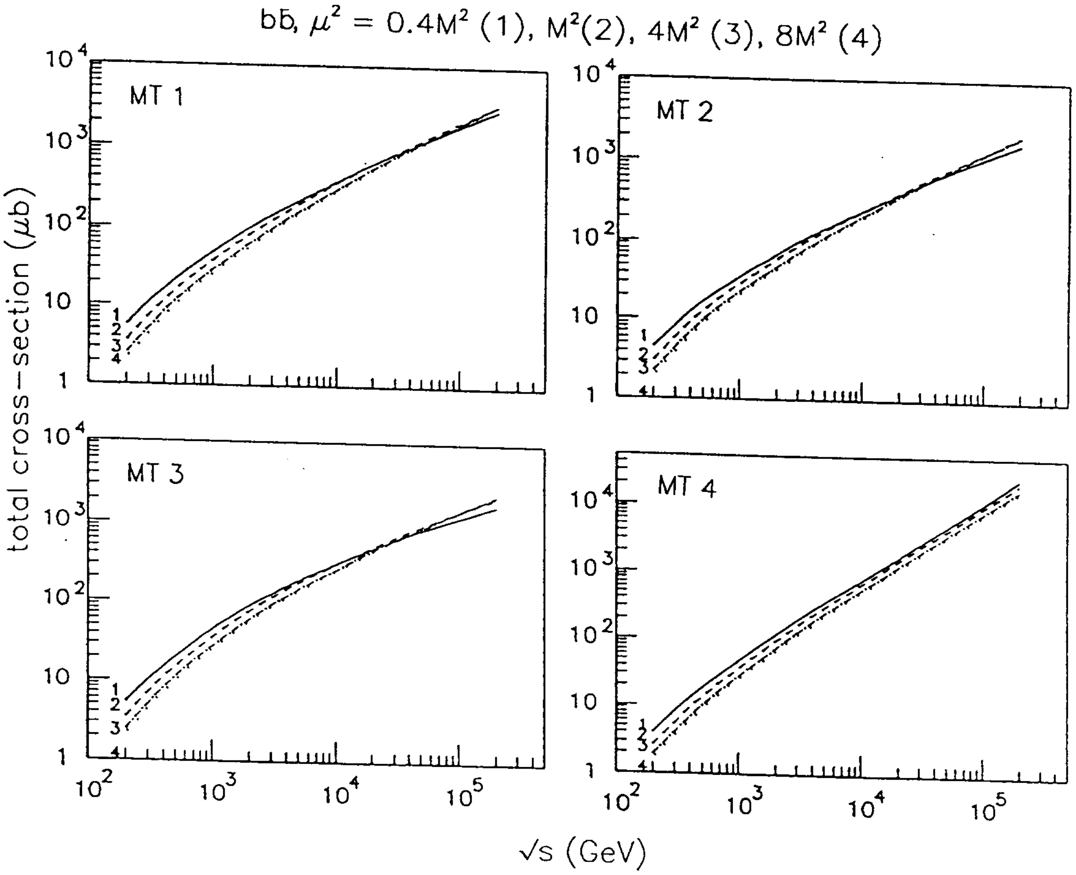

bb̄, μ² = 0.4M² (1), M²(2), 4M² (3), 8M² (4)
MT 1
MT 2
MT 3
MT 4
total cross-section (μb)
√s (GeV)

Fig.6

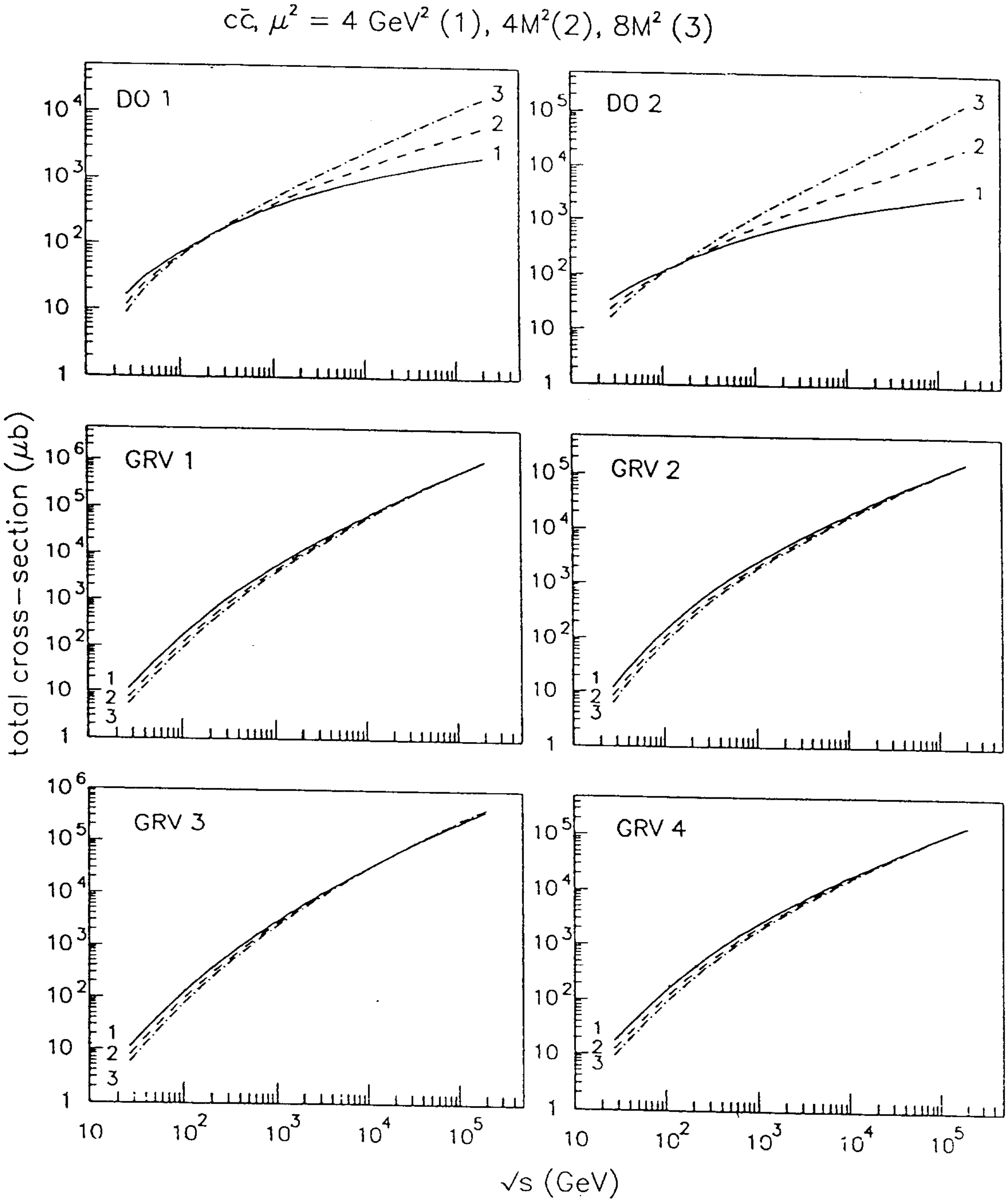
cc̄, μ² = 4 GeV² (1), 4M²(2), 8M² (3)
DO 1
DO 2
GRV 1
GRV 2
GRV 3
GRV 4
1
2
3
total cross-section (μb)
√s (GeV)
10
10²
10³
10⁴
10⁵
10⁶

Fig.7

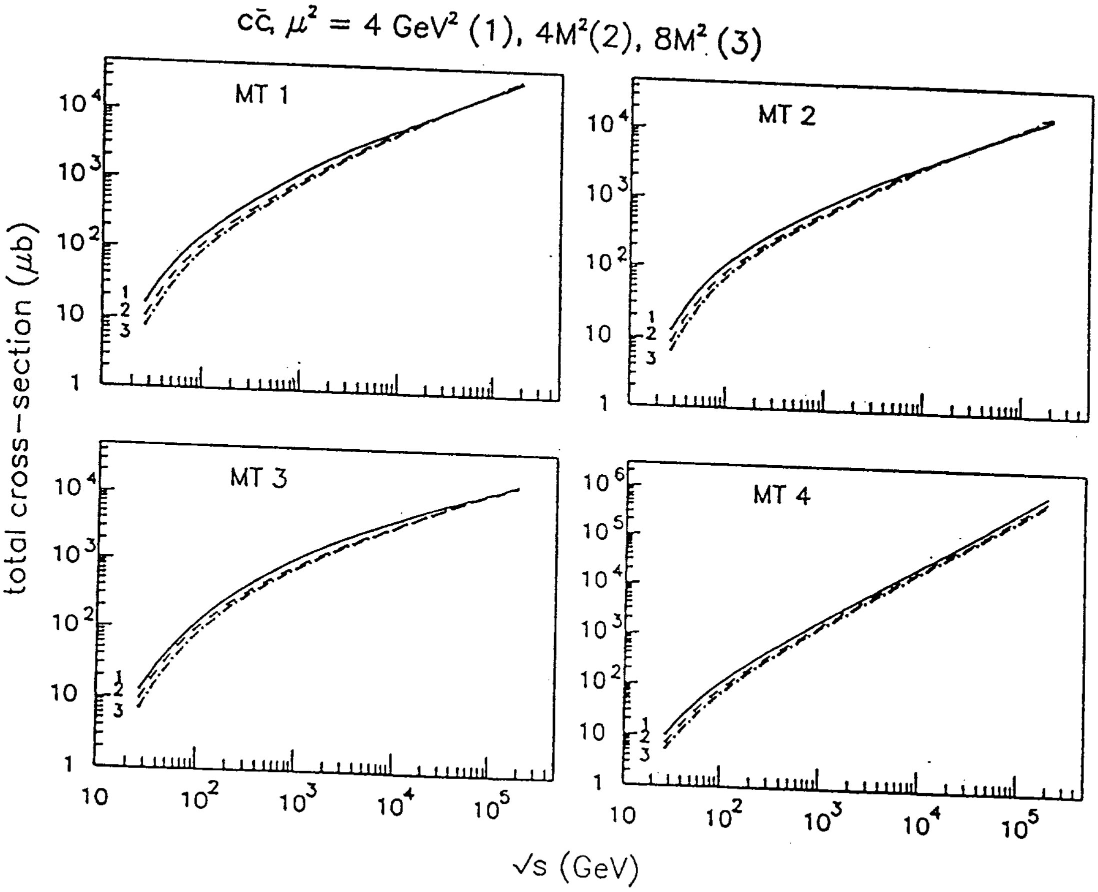

cc̄, μ² = 4 GeV² (1), 4M²(2), 8M² (3)
MT 1
MT 2
MT 3
MT 4
total cross-section (μb)
√s (GeV)

Fig.8

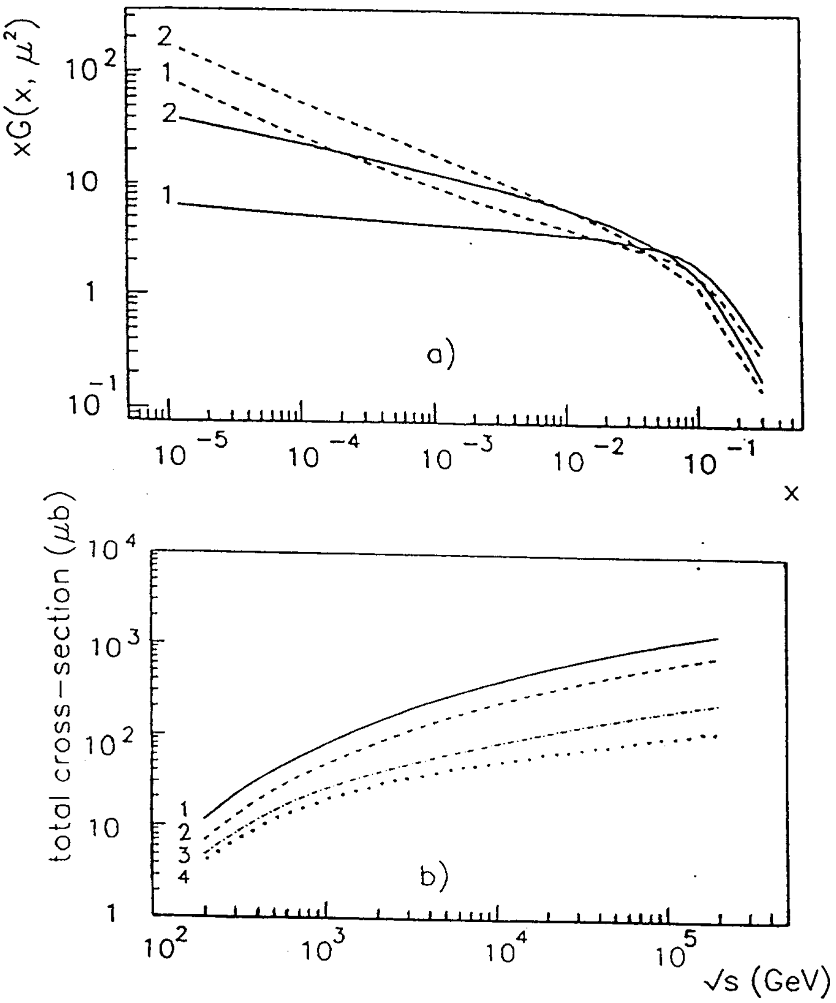

$xG(x, \mu^2)$
10^2
10
1
10^{-1}
2
1
2
1
a)
10^{-5}
10^{-4}
10^{-3}
10^{-2}
10^{-1}
x
total cross-section (μb)
10^4
10^3
10^2
10
1
1
2
3
4
b)
10^2
10^3
10^4
10^5
$\sqrt{s}$ (GeV)

Fig.9

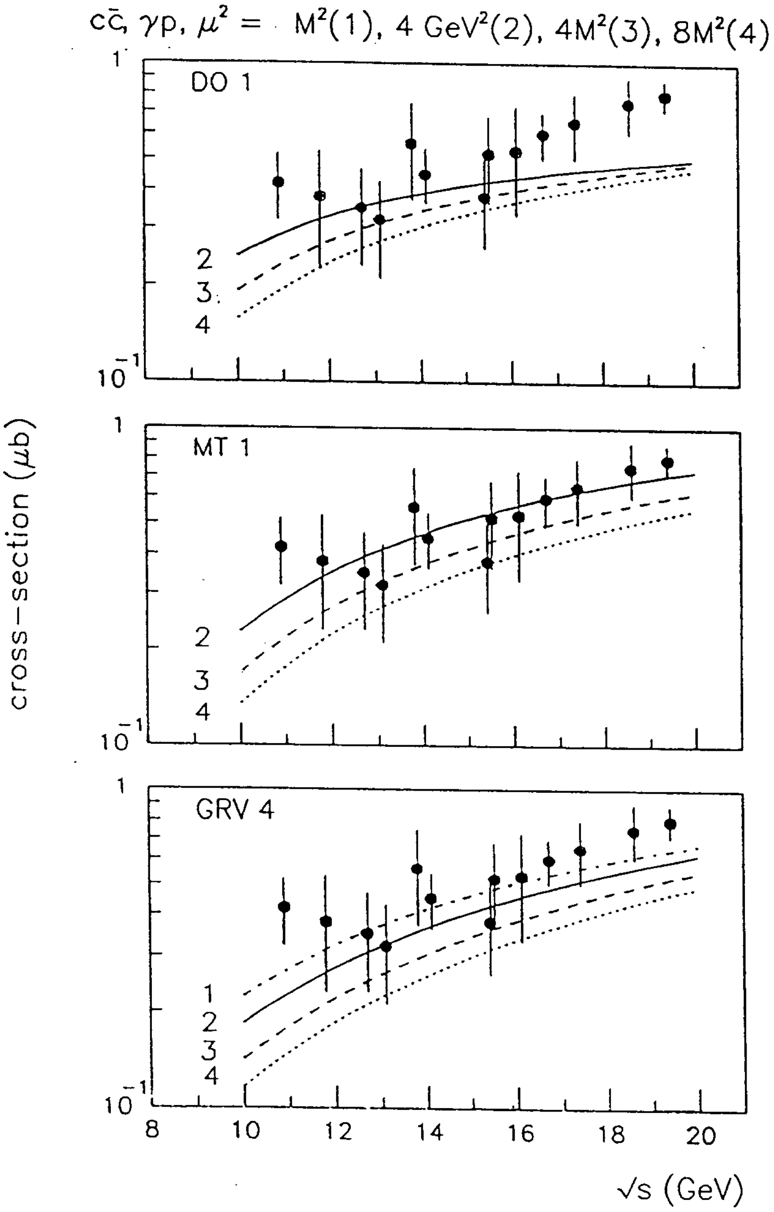
cc̄, γp, μ² = M²(1), 4 GeV²(2), 4M²(3), 8M²(4)
DO 1
MT 1
GRV 4
cross-section (μb)
√s (GeV)
1
10⁻¹
2
3
4
8
10
12
14
16
18
20

Fig.10

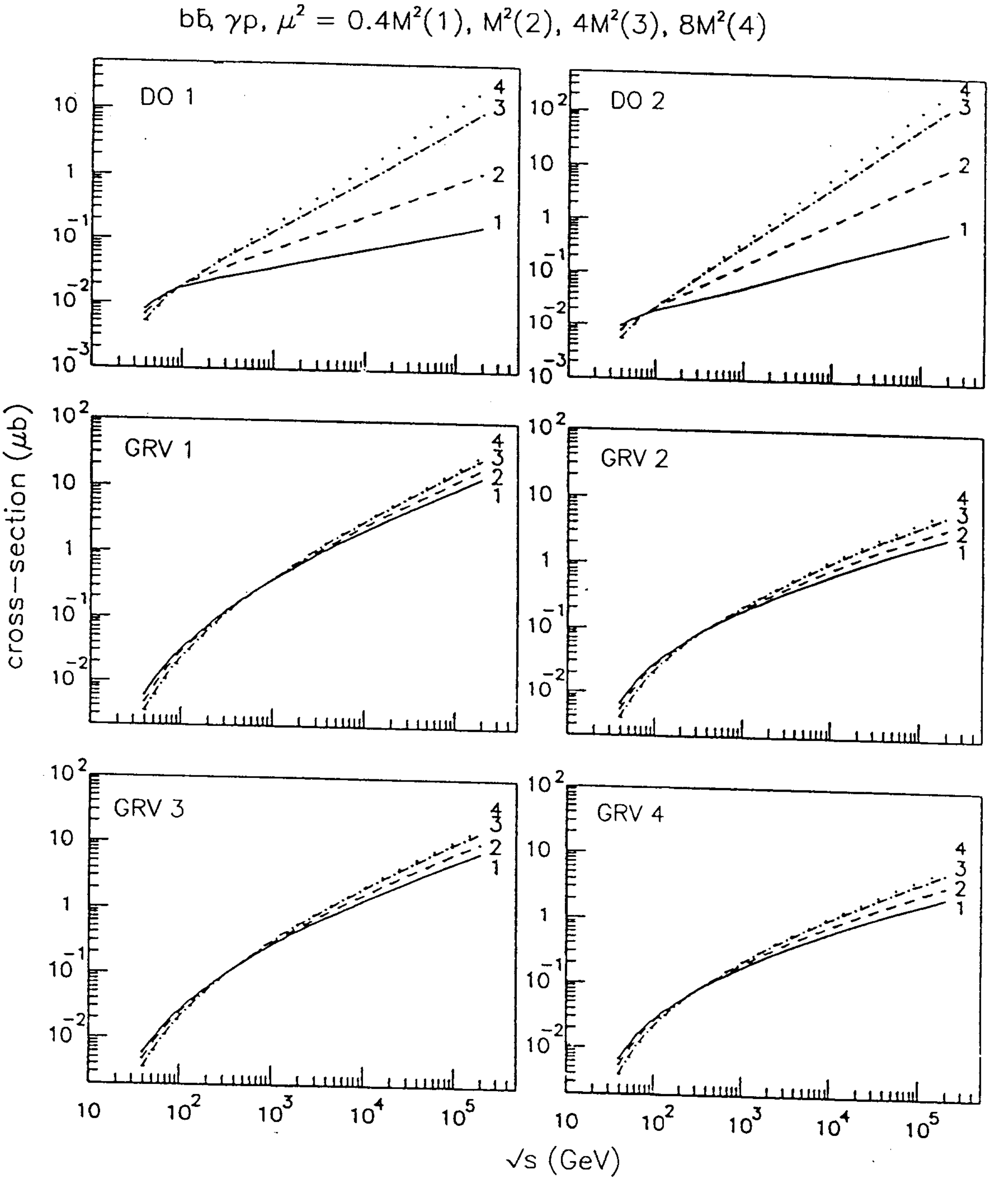
$b\bar{b}$, γp, $\mu^2 = 0.4M^2(1)$, $M^2(2)$, $4M^2(3)$, $8M^2(4)$
DO 1
DO 2
GRV 1
GRV 2
GRV 3
GRV 4
cross-section (μb)
$\sqrt{s}$ (GeV)

Fig.11

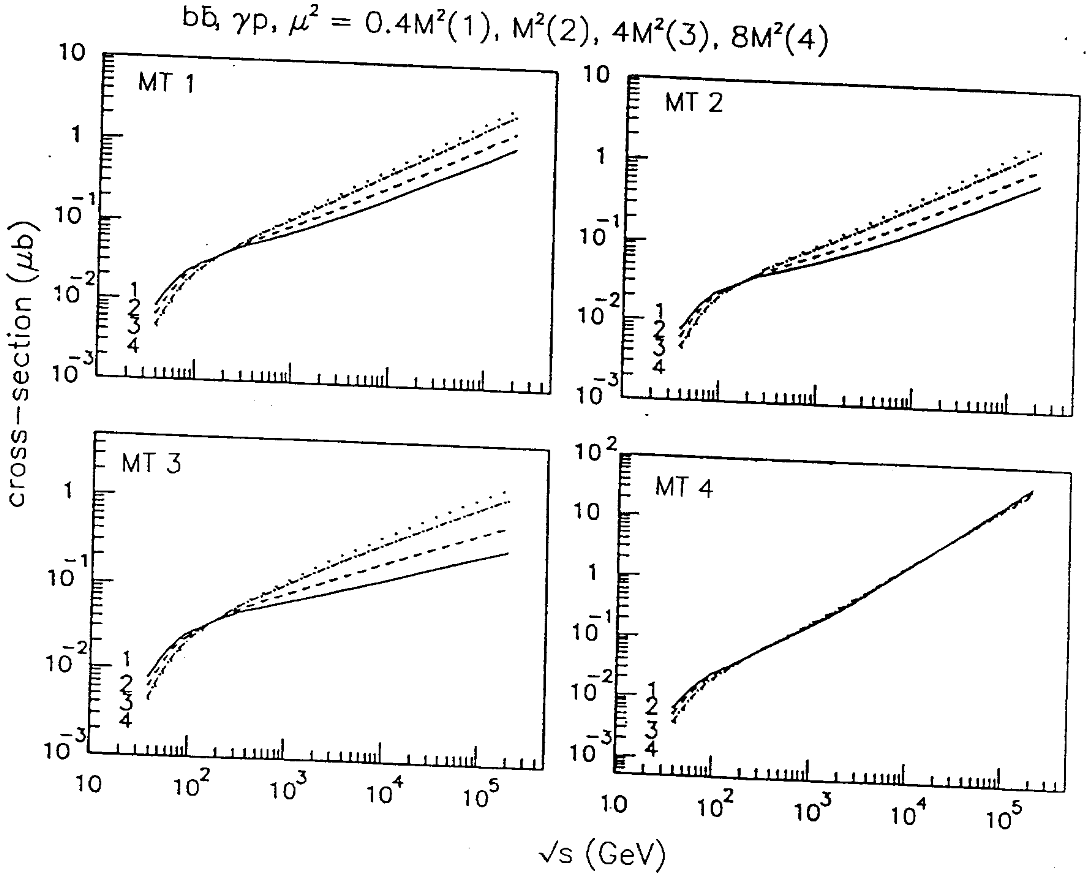

bb̄, γp, μ² = 0.4M²(1), M²(2), 4M²(3), 8M²(4)
MT 1
MT 2
MT 3
MT 4
cross-section (μb)
√s (GeV)
1
2
3
4

Fig.12

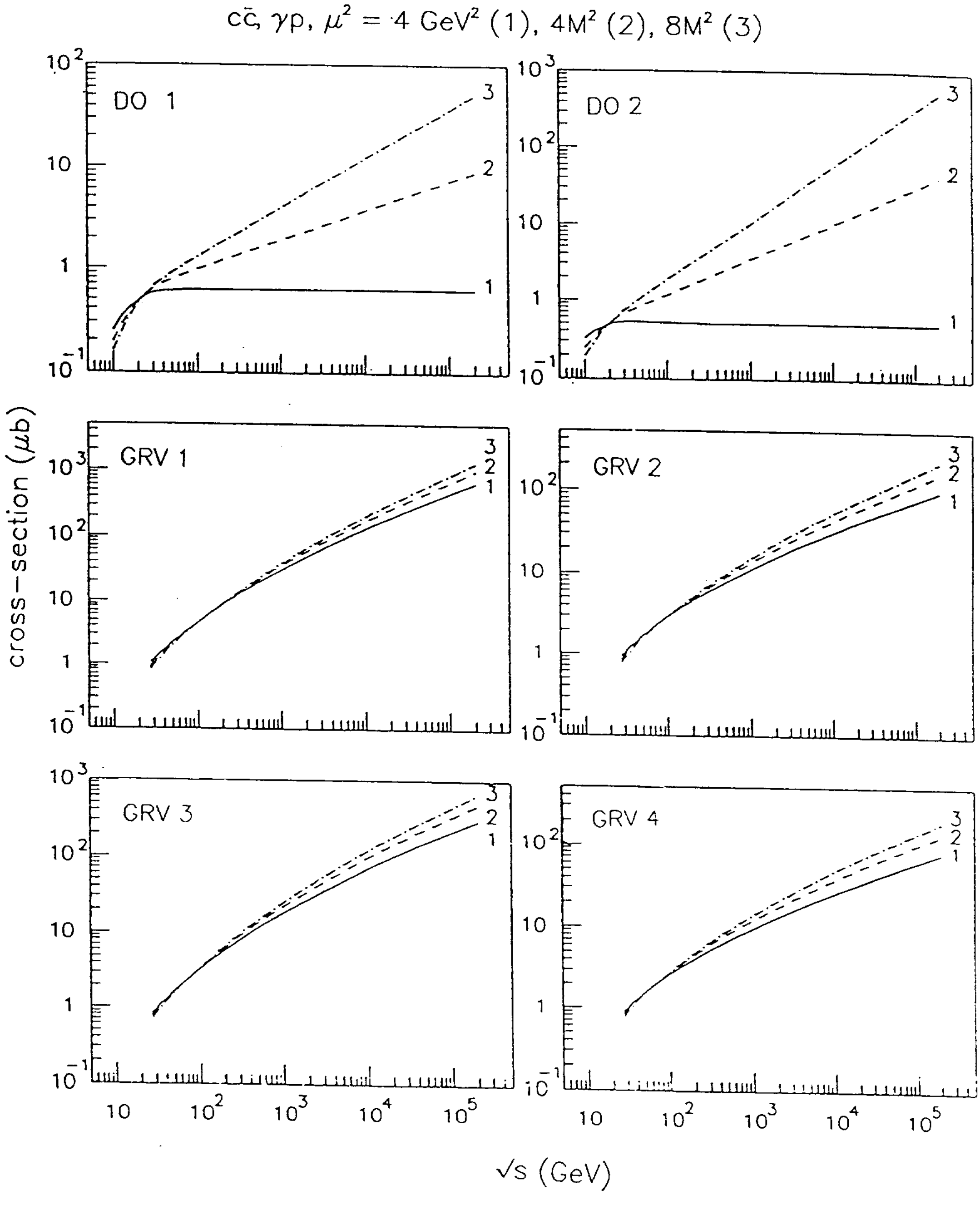

$c\bar{c}$, γp, μ^2 = 4 GeV² (1), 4M² (2), 8M² (3)
DO 1
DO 2
GRV 1
GRV 2
GRV 3
GRV 4
cross-section (μb)
√s (GeV)

Fig.13

$c\bar{c}$, γp, $\mu^2 = 4$ GeV^2 (1), $4M^2$ (2), $8M^2$ (3)

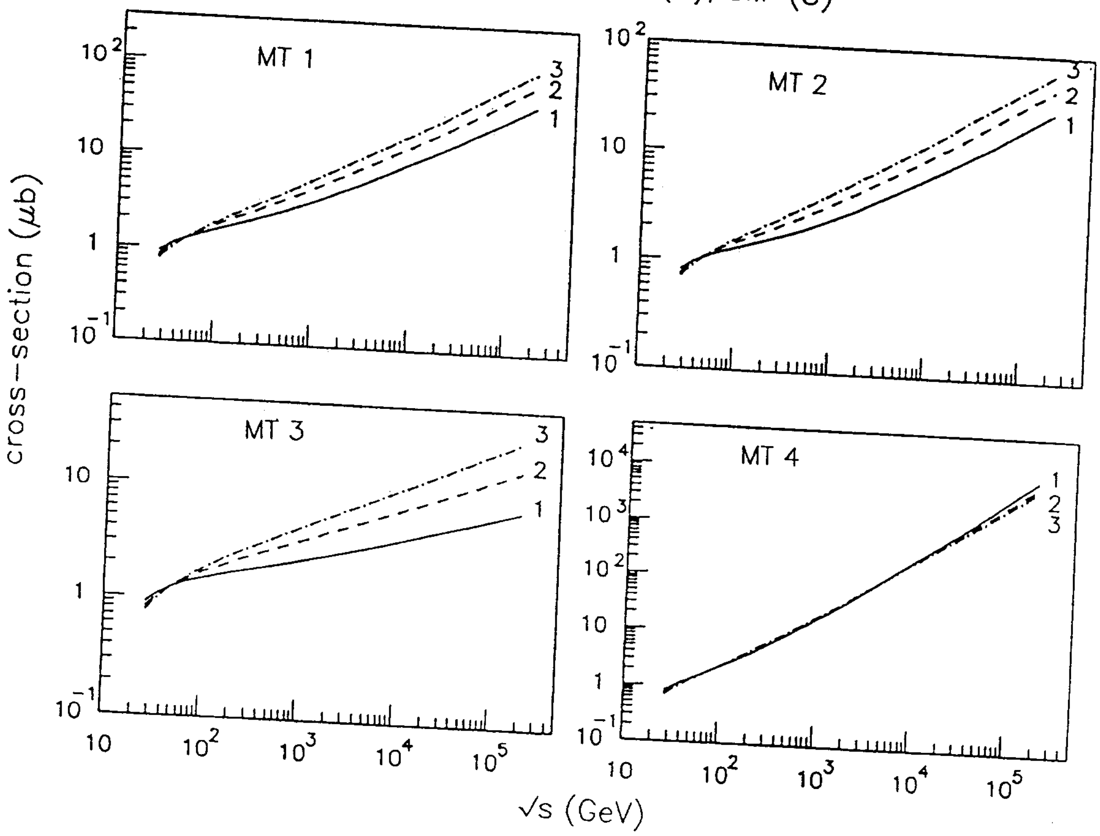

Fig.14

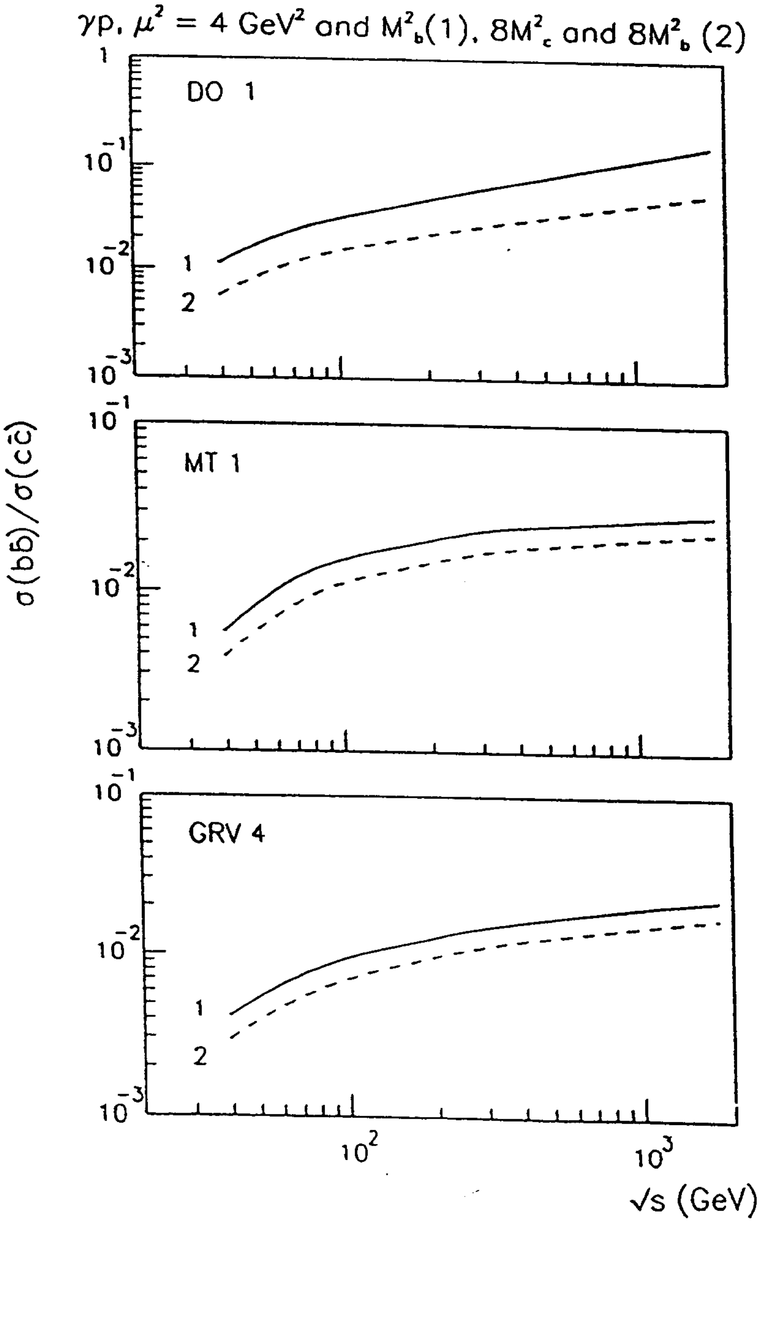

γp, μ² = 4 GeV² and M²_b(1), 8M²_c and 8M²_b (2)
DO 1
MT 1
GRV 4
1
2
σ(bb̄)/σ(cc̄)
√s (GeV)

Fig.15